*J. Weber**, *H.-P. Heim*

Institute of Material Engineering, Polymer Engineering, University of Kassel, Kassel, Germany

A Closer Look at the Bonding Capacity of Thick Metal-Plastic Hybrids

Metal-plastic hybrids have a lot of advantages compared to purely metal or purely plastic parts. A good design for metal-plastic hybrids can help to save weight, for example in automotive applications. Therefore, it is important to understand the joining mechanisms between both materials. Aluminum AlSi9Cu3(Fe) and polyamide 6.6 with 35 % glass fibers were used as joining partners. The materials were joined by enclosing the metal part at least partially with plastic right inside the injection molding tool. Afterwards, the tensile strength of the metal-plastic hybrids was tested under a quasi-static load. This article provides a short overview of publications related to this topic, and compares their conclusions with our own results. The focus is on the influence of the surface treatment on the metal part (shot-peening) and also the effects of different joining geometries within the bonding area. Statements made in other publications were able to be confirmed and expanded for shot-peened surfaces and particular joining geometries. In most cases, shot-peening the surface of metal parts is advantageous for the joining strength. If the strength of the bond is not important, but, instead, the achievable displacement is, a shot-peened surface is not always advantageous. In addition, the joining geometries have a large influence on the behavior of the part under static load.

1 Introduction

Hybrid Parts are very important for all fields of application. Due to their advantage – the systematic combination of properties of different kinds of materials – their importance will grow even more. The automotive sector, for example, wants to combine strong materials for structural functions with lightweight materials. There are numerous mechanisms for joining two materials and they always depend on the field of application, which defines important parameters, like the temperature range, the medium, the kind and quantity of the mechanical load, and the duration for all those parameters. In addition, the materials themselves have at least the same impact on the mechanism that determines how materials can be joined. An overview of recent technologies for joining PMH (polymer-metal hybrids) structures is available in various articles (Amancio-Filho and Dos Santos, 2009; Grujicic et al., 2008; Grujicic, 2014).

Irrespective of the many types of joining two or more materials to a hybrid part, one can classify them into three types of connection: the frictional connection, the form fit, and the adhesive bond or direct adhesion. The investigations for this article are based on a connection between a thermoplastic and aluminum. The thermoplastic material is a glass fiber reinforced polyamide 6.6. This is a material which is typically used for applications under the hood. Also, the mentioned aluminum can be found in many applications for cars, especially as die casting parts. A big problem of die casting aluminum is that it is not applicable for large parts with low wall thicknesses. Ostermann (2007) propagates a limit not smaller than 3 mm for those kinds of parts. The point is that mold cavities that are too thin cannot be filled with the molten metal, which means that those kinds of parts need to be designed with a stronger structure due to a processing issue, but not because of a stability issue. A combination of aluminum and plastic could help to solve this problem. The aluminum would impart a good level of stiffness, and the plastic could cover large areas of the component.

Since both materials are used for mass production, their price is low. Accordingly, the technique used to join them also needs to be cheap and suitable for mass production. Forming plastic requires an injection molding machine and tool. It would be cost-efficient to utilize this equipment to produce the joining between the plastic and the aluminum. Inserting the aluminum part into the injection molding tool and completely or partially enclosing it with the plastic melt would be the easiest method to achieve this. Apart from the many problems that come along with this joining technique, like a reliable tight lock between the tool and the die casting part, it is important to know how strong the bond between the aluminum and plastic can be. For this reason, research studies pertaining to this will be published with this article.

As for an adhesive bond between metals and plastic produced in the way described before, it was shown (Ehrenstein and Zhao, 2001; Zhao, 2002) that treating the surface primarily with chemical substances has a tremendous effect. The strength of the bond ranges between 0 N/mm^2 (simple cleaning of the metal before joining) and about 9 N/mm^2 (treating the aluminum with chromic acid). Even after an alternating climate test, consisting of 200 cycles with temperatures ranging between –40 °C and 80 °C, the strength of the bonding only decreased by a few percent.

* Mail address: Jonas Weber, Institute of Material Engineering, Polymer Engineering, University of Kassel, Mönchebergstraße 3, 34125, Kassel, Germany
E-mail: jonas.weber@web.de

In order to examine the influence of a form fit on the bonding strength, various research studies were performed (Eisler et al., 2010; Fleckenstein et al., 2012; Paul and Luke, 2010; Paul et al., 2012; Paul, 2013) on long glass fiber reinforced polyamide, which was co-molded together with the metal throughout the forming process. Different types of cut-out geometries were tested and compared. It was shown that the geometry or size of the cut-outs are not decisive, instead the amount of cut-outs within the joining area had the biggest impact on the pull-out force. Also, the influence of the pre-treatment on bonding strength was investigated. Corundum-treated surfaces showed better results than samples treated with different kinds of acids.

The focus of this publication is on the injection molding-based joining process that uses materials typically found in mass production. Therefore, the geometry of the joining area was chosen in a way that can be produced within the die casting process of the aluminum without requiring any further mechanical processing.

Table 2 shows the different categories of geometries investigated. Detailed information on the geometries of the specimens is provided in Fig. 6 to 9. Moreover, the surfaces of the samples were shot-peened because this is common practice in mass production, where a high number of the parts are shot-peened for deburring. The bearing area curves of an untreated surface and a shot-peened surface are compared in Fig. 5.

Before the experimental section details material, surface treatment, geometry, processing and testing, attention should be paid to the results of Eisler et al. (2010). Figure 1 shows the pull-out test of a specimen consisting of a steel insert which was pressed together with a compound based on polyamide 6.6 with long glass fibers. During the pull-out test, Eisler et al. (2010) differentiate between a first phase during which the mechanical load is carried only by the material-locking connection of the surface, which is also called direct adhesion. After a particular force is exceeded, the second phase starts in which the force is carried by the form-locking connection between the two materials. When the force reaches its maximum, the form-locking connection fails, and, therefore, the whole composite structure fails. Paul et al. (2014) states that for a good connection between metal part and plastic part it is not only necessary to have a good frictional connection, but to have a proper material-locking connection. The conclusion is based on the same investigations Eisler et al. (2010) performed. Paul et al. (2015) claims that there is no advantage for the mechanical behavior of the joint for static loading, when one of the joining mechanisms (direct adhesion by shot-peening or mechanical interlocking by geometry) is dominant. It was also stated that there will be advantageous effects under cyclic and creep loading.

In addition to other subjects, Zhao (2002) investigated the influence of different hole diameters on the pull-out behavior (Fig. 2). He describes the transition between the almost linear area and the subsequent non-linear area as the "Kniepunkt" [knee point] and the force at that point as "Kniekraft" [knee strength]. The knee point described by Zhao presumably corresponds to the area between the first and the second phase propagated by Eisler et al. (2010). The different position of both points may come from different designs of the specimens, the materials, and the process parameters. None of those publications allows conclusions about the behavior of specimens with a modified surface treatment or surface roughness to be made.

2 Experimental

2.1 Materials

The selection of the materials was based on possible applications of metal-plastic hybrids in the automotive industry, especially for usage under the hood, where there are particular requirements the materials have to meet: a temperature scale ranging from –40 °C up to 140 °C, high mechanical loads, and exposure to fluids like coolant, saltwater, fuel as well as oils for gears and engines. The aluminum die casting alloy AlSi9Cu3(Fe) was selected for this reason. In order to guarantee the chemical resistance against the mentioned fluids, mainly semi-crystalline plastics are used for those kinds of parts. Polyamide 6.6 is an often chosen as a compromise between temperature stability, low price, as well as processability. In addition to other factors, like the process parameters and roughness of the metal part, glass fibers within

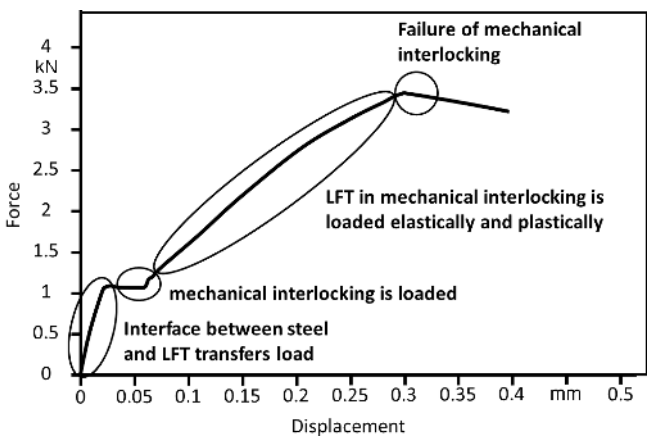

Fig. 1. Interpretation of a pull-out test based on Eisler et al. (2010)

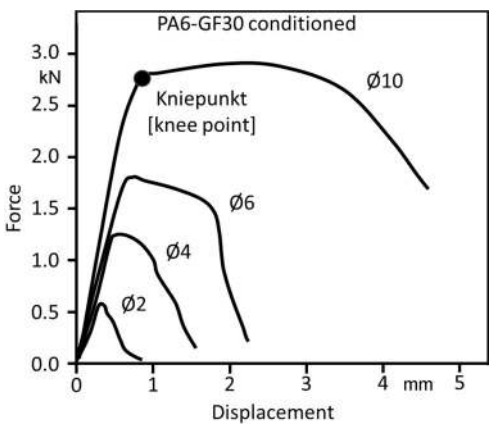

Fig. 2. Pull-out test with different interlocking diameters based on Zhao (2002)

the polymer matrix are very important for achieving a good connection between plastic and aluminum parts (Lucchetta et al., 2011). Thus, the mechanical and the joining performance can be increased by means of the addition of glass fibers. For this reason, polyamide 6.6 with the name Altech PA66 A 2035/507 from Albis Plastic GmbH, Hamburg, Germany, with 35 % short glass fibers content was chosen for the production of the hybrid test specimens. The glass fibers have a length of about 300 µm. All of the important attributes can be retrieved from the company's homepage: www.albis.com (2017).

2.2 Surface

A treated surface has a big influence on the joining potential between metal and plastic parts. For example, laser-structured surfaces show a much higher bonding force than untreated surfaces (Byskov-Nielsen, 2010; Byskov-Nielsen et al., 2010). Therefore, aluminum inserts with two different surfaces were utilized for the production of the hybrid test specimens: inserts without a special surface treatment and inserts with a shot-peened surface. Shot-peening is a common process for removing fine burrs and other residue from aluminum die casting parts. Such a surface treatment is already in use for a high percentage of die casting parts in series and is therefore not associated with higher costs. The shot-peening process for the inserts was exactly the same as for gearbox housings.

Table 1 contrasts the average surface roughness of the untreated surface with the shot-peened surface. As expected, the shot-peened surface has a substantially higher roughness than the untreated surface. Figure 3 and 4 show the surface scans made by a confocal laser microscope. The scaling of both images is identical so that the topological difference between both surfaces becomes clear. The bearing area curve in Fig. 5 was derived from both surface scans. It shows the height of the contour as a function of the bearing contact area ratio. While the earliest percentage of contact area of the untreated surface begins at a height of 35 µm, the earliest percentage contact area of the shot-peened surface begins at a height of 110 µm.

2.3 Geometry

To test the stability of the interlocking between the aluminum insert and the plastic, not only the surface of the insert was modified, but also its design. The geometry of the aluminum area, which will be in contact with the plastic, was varied. The external dimensions (Fig. 6 and 7) were identical for all specimens, because the injection molding tool (surrounding the insert) was always the same. The different geometries for the interlocking were classified into two categories (see Table 2). The "base geometry" (Fig. 6) was the root for further modifications, which are grouped in geometries with a "distinct undercut" and a "drill hole". All five geometries can be seen in Fig. 8 and 9.

Untreated Surface	R_Z = 11.5 µm
Shot-Peened Surface	R_Z = 73.3 µm

Table 1. Roughness of the aluminum surface

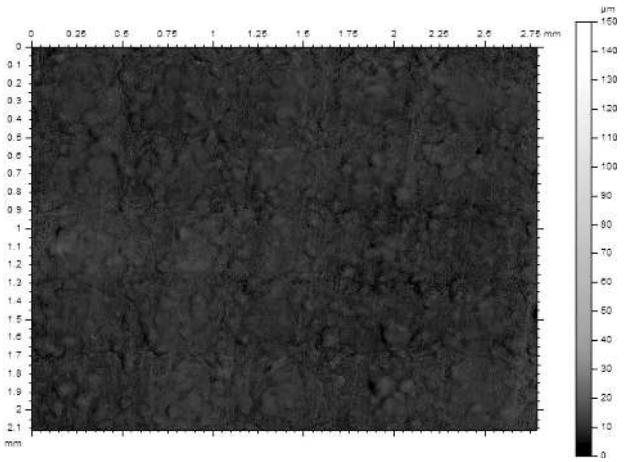

Fig. 3. Surface scan of aluminum specimen without surface treatment

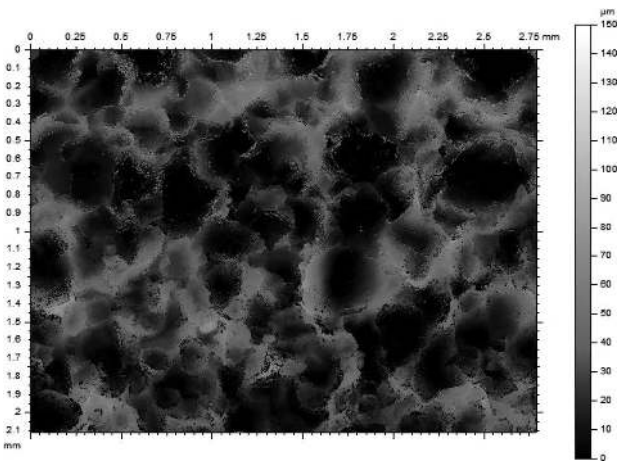

Fig. 4. Surface scan of aluminum specimen with shot-peened surface

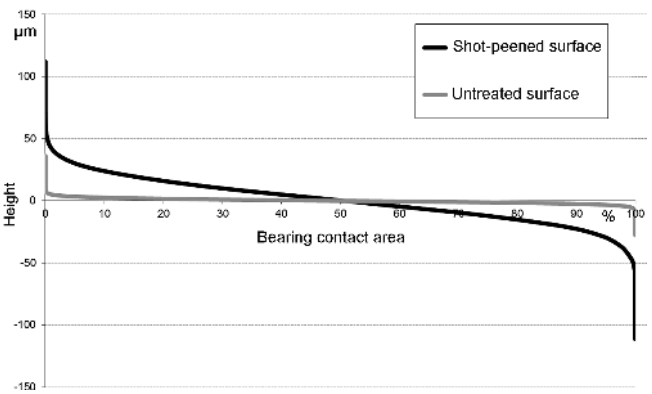

Fig. 5. Bearing area curves of a untreated aluminum surface and a shot-peened aluminum surface

2.4 Processing

An injection molding tool was used for the fabrication of the hybrid test specimens which was designed and manufactured only for this purpose. The tool has two cavities and was mounted on a vertical injection molding machine. The advantage of this type of machine is that the aluminum inserts do not need to be fixated with an additional mechanism. The inserts will be put in place before the molding process without any risk of moving or falling out. For the plastification of the thermoplastic, the granulate went through four temperature zones, starting with 280 °C in the first zone, 285 °C in the second zone, and 290 °C in the third and fourth zones. Also, the hot runner was operated at a temperature of 290 °C. The tool as well as the aluminum inserts before they were put into the cavities were tempered to 80 °C. A high temperature of the metal insert (Ramani and Moriarty, 1998; Zhao, 2002), a high holding pressure (Zhao, 2002) as well as a low viscosity of the plastic during the injection molding process (Ramani and Tagle, 1996) are essential factors for a good bonding capacity between both materials. A low tooling temperature and a long cooling time have a positive influence on the warpage of hybrid structures (Zhao, 2002) and so probably have a positive influence on the bonding strength. The flow rate for the injection of the plastic into the cavity was set to 70 cm^3/s. The holding pressure was 400 bar for 8 s, 250 bar for 4 s, and 100 bar for another 4 s. The injection cycle ended with a cooling time of 20 s. Figure 10 shows the complete set of test specimens with polycarbonate for demonstration purposes and with polyamide 6.6 for test purposes.

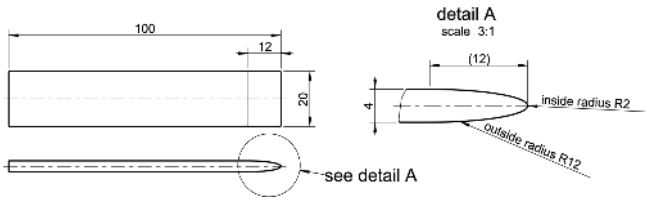

Fig. 6. Base geometry of the aluminum insert for pull-out test

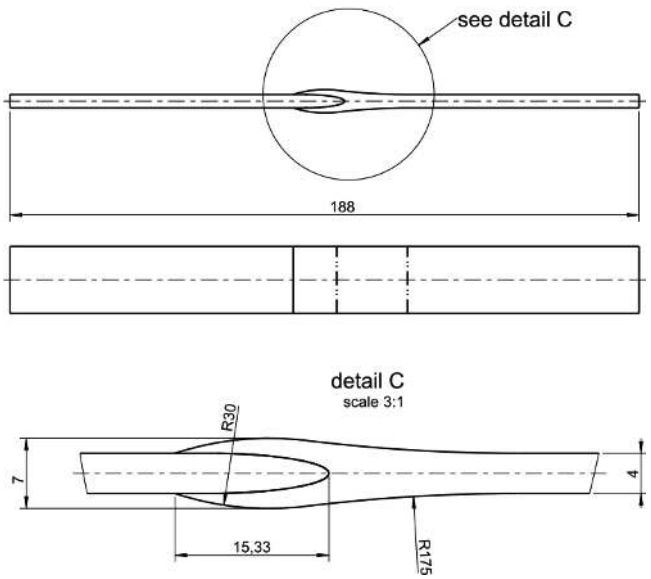

Fig. 7. Assembly of aluminum insert and plastic

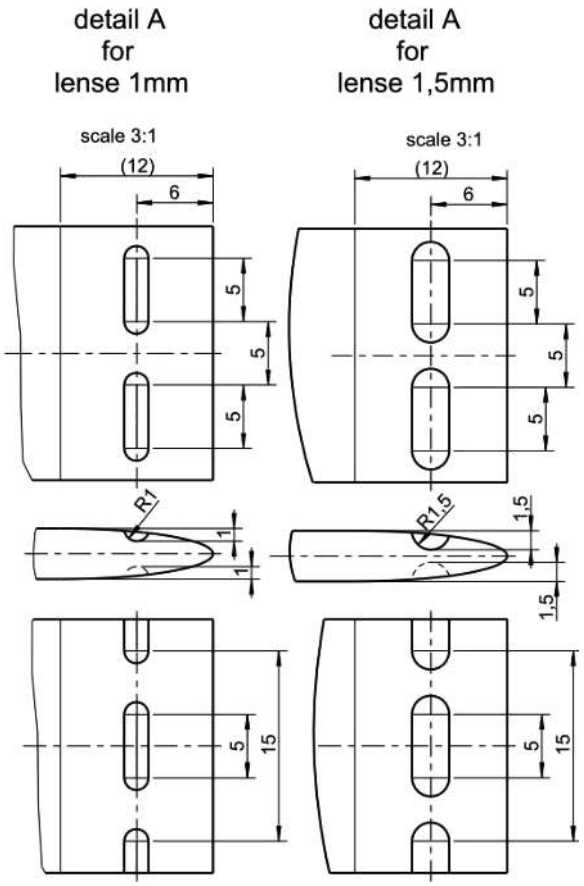

Fig. 8. Geometry for specimen with lenses (1 mm and 1.5 mm)

Base	Category	Geometry
Base geometry (see Fig. 6)	Distinct undercut (see Fig. 8)	Lens 1 mm Lens 1.5 mm
	Drill hole (see Fig. 9)	5 mm diameter 2 × 5 mm diameter 6 mm diameter

Table 2. Classification of different geometries used for the pull-out test

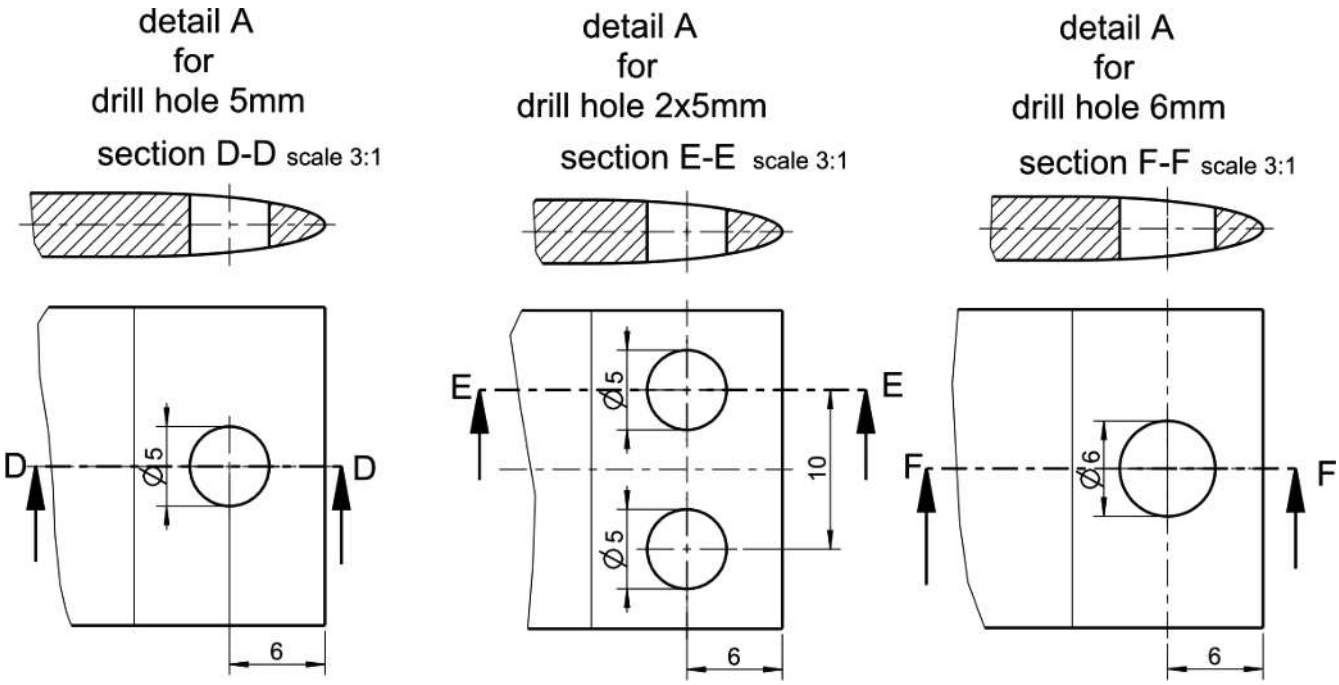

Fig. 9. Geometry for specimen with drill hole (5 mm, 2 × 5 mm and 6 mm diameter)

2.5 Testing

The tensile tests were performed with a standard tensile testing machine under standardized conditions (standard atmosphere 23/50 class 2 according to ISO 291). The execution of the tensile tests follows the norm for tensile tests (DIN EN ISO 527). For the determination of the displacement, a clip-on extensometer with a measurement range of 50 mm was used. The testing speed was 1 mm/min. The clamping length of the specimens was 120 mm. At least five specimens for each design of the interlocking geometry and each version of the surface treatment were tested. The results in section 3 show a representative curve for each configuration. To achieve better comparability between the specimens, they were tested right after injection molding without conditioning of the polyamide.

Fig. 10. Metal-plastic specimens with polycarbonate (transparent) for demonstration and polyamide (black) for tensile tests

3 Results and Discussion

The mean value for the maximum pull out force (F_{MAX}) of all five specimens for each geometry are shown in Fig. 11. Also the standard deviation can be seen from this figure. The results for each type of geometry will be discussed separately below.

The fracture behavior of selected specimen is shown in Fig. 12, Fig. 13, and Fig. 14. It is distinguishable from all pictures that the plastic got torn off form the metal surface without leaving remains. The fracture behavior is the same for all tested geometries irrespective of the surface treatment.

Figure 15 shows the pull-out test of specimens with a lens geometry (1 mm). The specimen with the untreated surface shows the transition between the material-locking and the form-locking area at about 450 N (F_S). In the case of the untreated curve, it must be assumed that the specimen only has a limited ability to transfer the load by means of material-locking. The mechanical load is transferred by form-locking shortly after the start. It is evident that the specimen with the shot-peened surface shows no transition (F_S) between the material-locking and the form-locking, and displays sudden failure at about 2 100 N. It can be assumed that the capability of load transferring of a certain geometry is almost independent of the surface treatment. So, while $F_{S\ SHOT\text{-}PEENED}$ exceeds the load-bearing capacity of the form-locking portion, the composite structure fails abruptly subsequently.

The two marked areas show the range of F_S for untreated surfaces (dotted area with low intensity) and shot-peened surfaces (dotted area with high intensity) for all tested geometries.

- The range of $F_{S\ UNTREATED}$ starts at 200 N and ends at 500 N.
- The range of $F_{S\ SHOT\text{-}PEENED}$ starts at 2000 N and ends at 2 600 N.

The same comparison with a bigger geometry (lens geometry 1.5 mm) is shown in Fig. 16. The almost identical maximum

force (F_{MAX}) for the untreated and the shot-peened surface is noticeable. Also, it would seem that the specimen with the untreated surface has no or only limited ability to transfer any load by material-locking ($F_{S\ UNTREATED} \approx 250$ N). The mechanical load is transferred by form-locking nearly from the start. Therefore, one can deduce from the curves that the lens geometry (1.5 mm) with an untreated surface has the same load transferring abilities as a shot-peened surface with the same geometry. If the mechanical load is induced by the position and not the force, a shot-peened surface would have a negative effect because it would result in failure at an earlier point of displacement.

The next comparison of force displacement diagrams is shown in Fig. 17, and constitutes two curves with a drill hole geometry of 6 mm and either an untreated surface or a shot-peened surface. The material-locking of the specimen with the untreated surface already failed at a minor load at about 200 N and subsequently transferred all forces by form-locking of the drill hole geometry. The drill hole geometry encourages shrinkage of the plastic during injection molding towards the metal surface. Due to the strong direct adhesion between the metal and the plastic caused by the shrinkage and the shot-peened surface, the transition between material-locking and form-locking is at the upper limit of the area determined for $F_{S\ SHOT\text{-}PEENED}$. Since the load bearing capacity of the drill hole

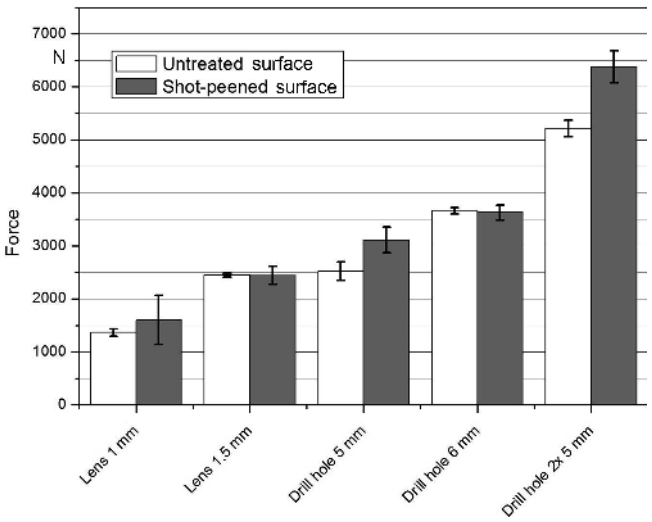

Fig. 11. Mean value and standard deviation for F max

Fig. 12. Fracture behavior of 1 mm lens geometry with shot-peened surface

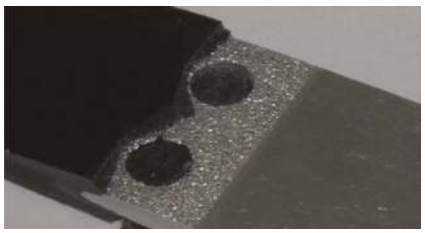

Fig. 13. Fracture behavior of 2 × 5 mm hole geometry with shot-peened surface

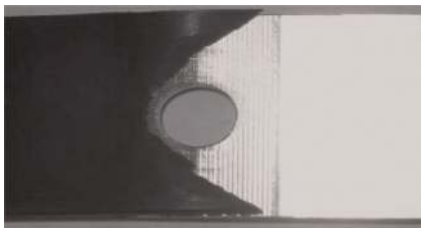

Fig. 14. Fracture behavior of 5 mm hole geometry with untreated surface

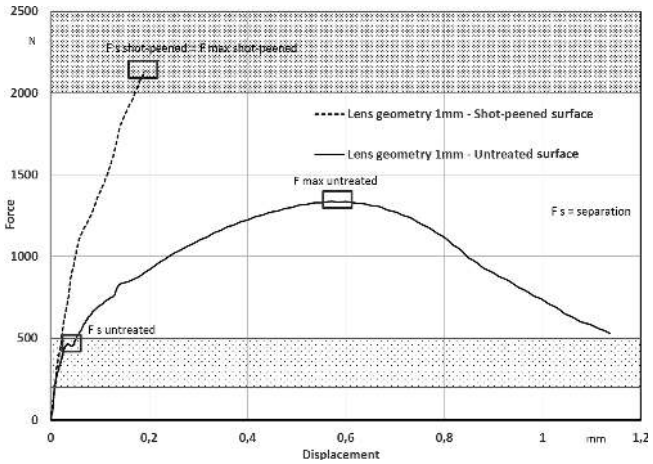

Fig. 15. Comparison between shot-peened and untreated aluminum surface of specimens joined with a lens geometry of 1 mm

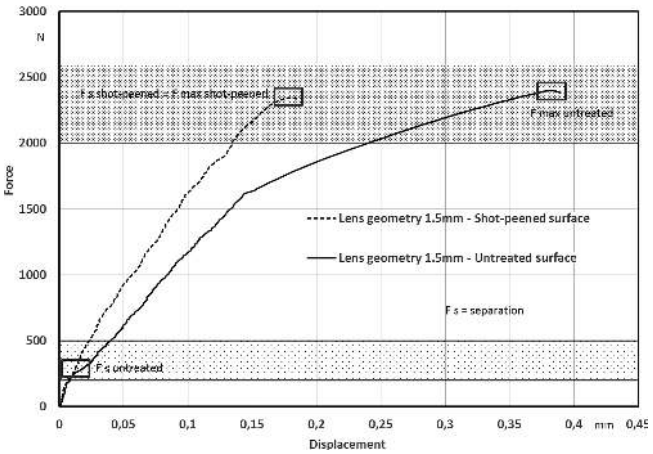

Fig. 16. Comparison between shot-peened and untreated aluminum surface of specimens joined with a lens geometry of 1.5 mm

geometry is independent of the type of surface treatment, the failure of both specimens occurs in the same range of force. Like the specimens with the 1.5 mm lens geometry from Fig. 16, the specimen here with the untreated surface can also bear a higher level of displacement before failure.

The force displacement graphs for the untreated and the shot-peened specimens with a 2×5 mm drill hole geometry are shown in Fig. 18. Also, it becomes apparent here that only a small load ($F_{S\ UNTREATED} \approx 500$ N) is necessary to loosen the material-locking of an untreated surface, and, furthermore, only the form-locking transfers all the load. In contrast to the specimen with the 6 mm drill hole geometry, the shot-peened surface shows a soft transition from the material-locking zone to the form-locking zone at about 2 600 N. Also, the difference in the maximum forces between the untreated and the shot-peened surface indicates that not only the form-locking bears the entire load for the shot-peened surface. Otherwise, the maximum forces for both kinds of surface should almost be identical. Surprisingly, this is the first specimen where the shot-peened surface can bear a higher displacement than the specimen with the untreated surface.

The comparison of both surface types for the specimens with a 5 mm drill hole geometry is shown in Fig. 19. Similar to the specimen with a 6 mm drill hole geometry, the untreated surface causes the failure of the material-lock at an early state ($F_{S\ UNTREATED} \approx 200$ N). The maximum force, which can be transferred by form-lock, is unsurprisingly lower ($F_{MAX\ UNTREATED} \approx 2\,400$ N for 5 mm diameter) than the one of the specimen with the 6 mm drill hole geometry in Fig. 17 ($F_{MAX\ UNTREATED} \approx 3\,600$ N for 6 mm diameter). The same applies to the shot-peened specimens in Fig. 17 ($F_{MAX\ SHOT\text{-}PEENED} \approx 3\,600$ N for 6 mm diameter) and Fig. 19 ($F_{MAX\ SHOT\text{-}PEENED} \approx 3\,300$ N for 5 mm diameter). An essential difference is that for this geometry the specimens with the shot-peened surface can bear a higher displacement (just like the specimens with the 2×5 mm drill hole geometry). In general, it can be said that the behavior of the specimens with one and two drill holes each 5 mm in diameter are qualitatively identical, and, also, the transition between material-locking and form-locking is very smooth for both geometries. A big difference is evident when comparing it with the specimen with the drill hole geometry measuring 6 mm. The high force level leads to an alignment of the maximum force for both types of surface treatment. The shot-peened surface loses its general benefit that is based on the additional material-locking.

Figure 20 summarizes all the results from Fig. 15 to 19 and outlines the transition of the pull-out behavior from an untreated surface (left diagrams) to a shot-peened surface (right diagrams). Phase I represents the section with mainly load transfer by surface adherence and minor load transfer by mechanical interlocking. Phase II represents the section with minor load transfer by surface adherence and mainly load transfer by mechanical interlocking. Phase III only has load transfer by mechanical interlocking.

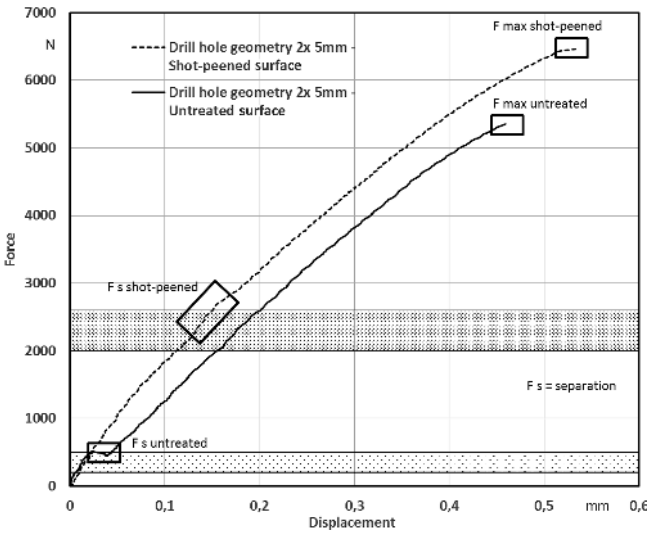

Fig. 18. Comparison between shot-peened and untreated aluminum surface of specimens joined with a drill hole geometry of 2×5 mm

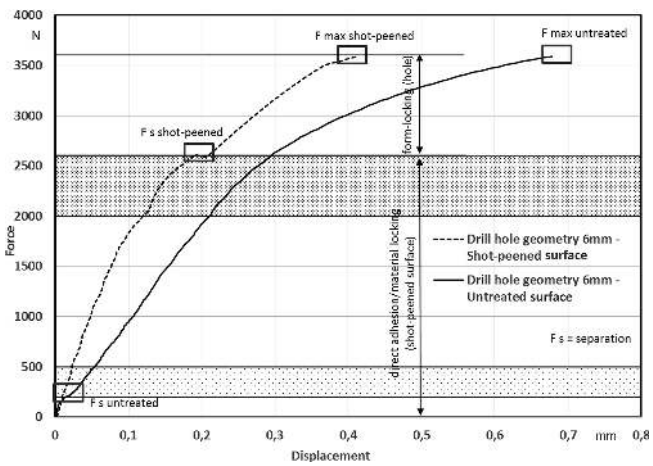

Fig. 17. Comparison between shot-peened and untreated aluminum surface of specimens joined with a drill hole geometry of 6 mm

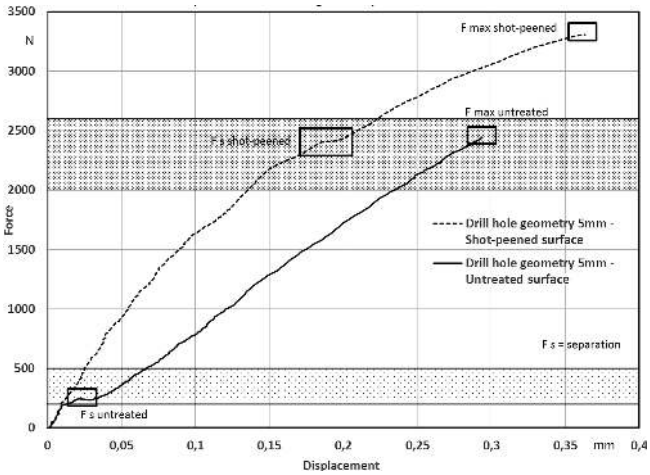

Fig. 19. Comparison between shot-peened and untreated aluminum surface of specimens joined with a drill hole geometry of 5 mm

4 Conclusions

The following conclusions can be drawn from the presented test results:

- In all cases, the maximum forces of the specimens with a shot-peened surface are at least as high as the ones of the specimens with untreated surfaces.
- Compared to an untreated surface a shot-peened surface will increase the standard deviation for F_{MAX}. So the results will vary more with a shot-peened surface than with an untreated surface. This may be caused by a more irregular surface structure which acts as an initial point for crack growth.
- The shot-peened surfaces of the specimens lead to a higher gradient of the force displacement curve in all geometries compared to specimens with untreated surfaces.
- If $F_{MAX\ UNTREATED} \approx F_{MAX\ SHOT\text{-}PEENED}$ (e. g. 1.5 mm lens geometry and 6 mm drill hole geometry,) the achievable displacement until failure of shot-peened specimens is smaller than that of untreated specimens.
- If a high maximum force is pursued, the shot-peening process is always advantageous.
- If a high maximum displacement is pursued, the shot-peening process is not always advantageous. Only geometries that achieve a large gain in their maximum force when going from an untreated to a shot-peened surface can also benefit from an increased maximum displacement (e. g. 5 mm drill hole and 2×5 mm drill hole geometry).
- In general, the shot-peening process has an impact on the distribution of phase I and phase III. The shot-peening shifts the proportion towards phase I, and, in extreme cases, phase III disappears entirely (Fig. 20).

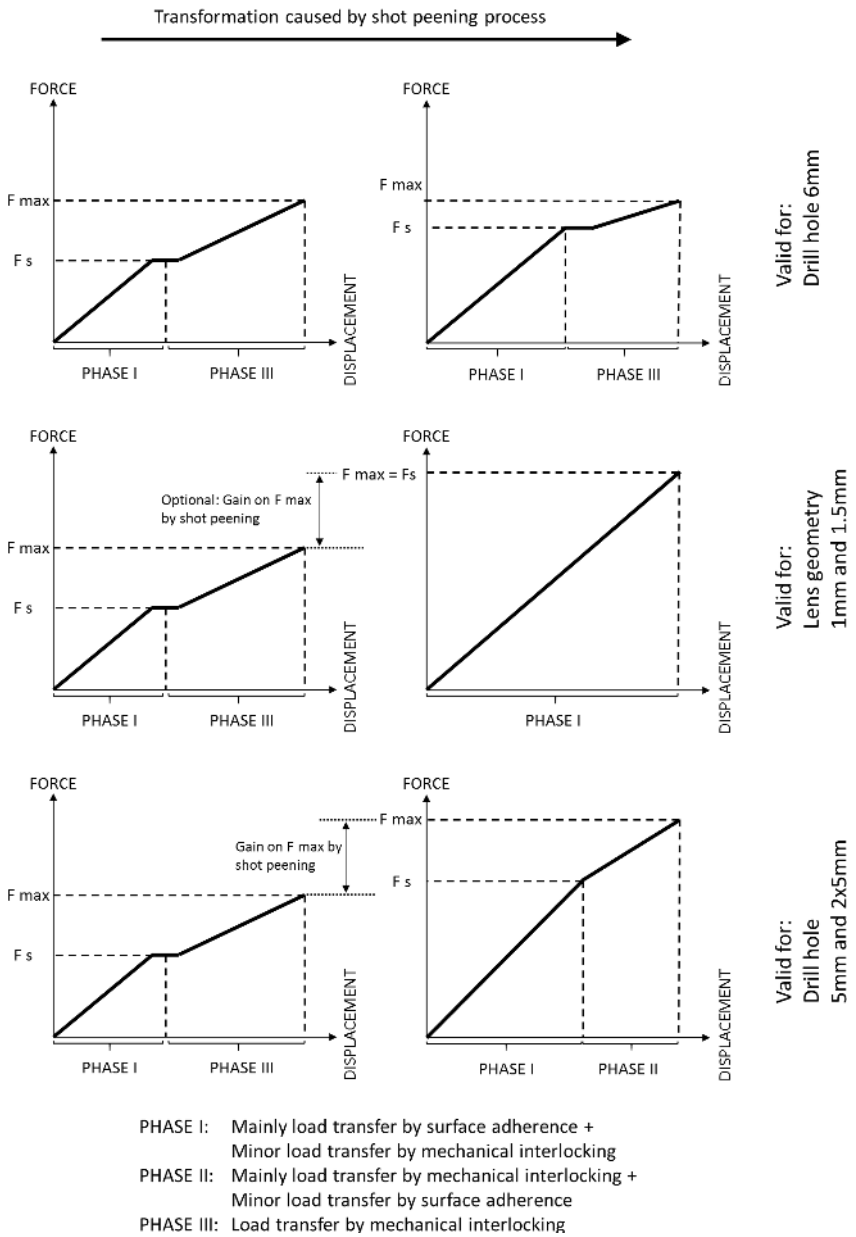

Fig. 20. Transformation of the force displacement graph as a result of the shot-peening process

- Shot-peened geometries belonging to the category "distinct undercut" according to Table 2 can be allocated to the middle diagrams (Fig. 20), while shot-peened geometries belonging to the category "drill hole" can be allocated to the top diagrams (6 mm) and the bottom diagrams (5 mm and 2x 5 mm). This indicates that specimens with a weaker geometry for mechanical interlocking no longer show a transition from phase I to phase III, but remain in phase I until failure occurs when they become shot-peened.
- The fact that for the 5 mm drill hole and the 2x 5 mm drill hole $F_{MAX\ SHOT\text{-}PEENED}$ is higher than $F_{MAX\ UNTREATED}$ seems to be unreasonable since $F_{S\ SHOT\text{-}PEENED}$ is visible in both diagrams (Fig. 18 and 19). Upon closer examination, it becomes clear that the occurrence of $F_{S\ SHOT\text{-}PEENED}$ is much more weaker than in the 6 mm drill hole specimen. Therefore, it seems that the transition from phase I to phase III while passing F_S is not performed completely in the specimen with 5 mm diameter geometries. Thus, it must be assumed that there is still a minor load transfer caused by surface adherence (phase II) after $F_{S\ SHOT\text{-}PEENED}$.
- The approach of Eisler et al. (2010) to divide the pull-out process into two different phases (phase I and phase III) can be confirmed and extended to specimens with a shot-peened surface. In certain situations, the proportions of the two phases shift in a way that only one phase remains (valid for 1 mm and 1.5 mm lens geometries with a shot-peened surface) or the transition from one phase to the other phase is not achieved completely, and an intermediate phase (phase II) occurs (valid for 5 mm and 2×5 mm drill hole geometries with shot-peened surface). As a result, the conclusion drawn by Paul et al. (2014) is correct. Also, the thesis by Paul et al. (2015), which states that there will be no gain in structural strength when one of the bonding mechanisms is dominant, was confirmed by the 6 mm drill hole geometry. If the mechanical interlocking itself is so strong that it exceeds the gained structural strength made by shot-peening, the effect of shot-peening is lapsed.
- The behavior postulated by Zhao (2002) with the occurrence of a knee point cannot be retraced in that manner. An essential difference is that Zhao used conditioned specimens while the specimens in these tests were used right after injection molding, which would explain the absence of a knee point. Due to the fact that the knee point shows such a significant change in the force displacement curve, the only plausible conclusion is that it is identical to the transition between the first and the second phases (F_S). The differences in the curves must come from imparities caused by material, process and/or testing.
- The statement by Paul et al. (2015) that the cyclic and creep behavior of joints with direct adhesion and form-locking would benefit could not be proven, because those types of tests were not performed. Such test results, especially those obtained with a 6 mm drill hole geometry or similar geometry, will be innovative for future investigations.

References

Amancio-Filho, S. T., Dos Santos, J. F., "Joining of Polymers and Polymer-Metal Hybrid Structures: Recent Developments and Trends", Polym. Eng. Sci., **49**, 1461 – 1476 (2009), DOI:10.1002/pen.21424

Byskov-Nielsen, J., "Short-pulse Laser Ablation of Metals: Fundamentals and Applications for Micro-mechanical Interlocking", PhD Thesis, Department of Physics and Astronomy, University of Aarhus, Aarhus (2010)

Byskov-Nielsen, J., Boll, J. V., Holm, A. H., Højsholt, R. and Balling, P., "Ultra-High-Strength Micro-Mechanical Interlocking by Injection Molding into Laser-Structured Surfaces", Int. J. Adhes. Adhes., **30**, 485 – 488 (2010), DOI:10.1016/j.ijadhadh.2010.03.008

Ehrenstein, G. F., Zhao, G., "Kunststoff-Metall-Hybridtechnik", Zeitschrift für wirtschaftlichen Fabrikbetrieb, **96**, 132 – 137 (2001)

Eisler, H., Reif, M. and Henning, F., "Investigation on the Mechanical Behaviour of Hybrid Polymer Metal Joints", 14th European Conference on Composite Materials, Budapest (2010)

Fleckenstein, J., Paul, H., Luke, M. and Büter, A., „Ermittlung der mechanischen Eigenschaften von Langfaserverstärkten Thermoplasten (LFT) auch im Hinblick auf den Einsatz in Materialverbünden", Conference DVM Tag 2012 – Multimaterialsysteme, Berlin (2012)

Grujicic, M., Sellappan, V., Omar, M. A., Seyr, N., Obieglo, A., Erdmann, M. and Holzleitner, J., "An Overview of the Polymer-to-Metal Direct-Adhesion Hybrid Technologies for Load-Bearing Automotive Components", J. Mater. Process. Technol., **197**, 363 – 373 (2008), DOI:10.1016/j.jmatprotec.2007.06.058

Grujicic, M., "Injection Over Molding of Polymer-Metal Hybrid Structures", American Journal of Science and Technology, **1**, 168 – 181 (2014)

Lucchetta, G., Marinello, F. and Bariani, P. F., "Aluminum Sheet Surface Roughness Correlation with Adhesion in Polymer Metal Hybrid Overmolding", CIRP Annals – Manufacturing Technology, **60**, 559 – 562 (2011), DOI:10.1016/j.cirp.2011.03.073

Ostermann, F.: Anwendungstechnologie Aluminium, 2nd Completely Revised and Updated Edition, Springer, Berlin (2007)

Paul, H., Luke, M., "Langfaserverstärkte Kunststoff-Metall-Hybridverbunde – Bewertung des Verformungs- und Versagensverhaltens", Konstruktion, **9**, 11 – 12 (2010)

Paul, H., Luke, M. and Henning, F., "Evaluation of the Joining Mechanisms of Polymer Metal Composites", 15th European Conference on Composite Materials, Venice (2012)

Paul, H., Luke, M. and Henning, F., "Kunststoff-Metall-Hybridverbunde – Experimentelle Untersuchungen zum Verformungs- und Versagensverhalten", Kunststofftechnik, **10**, 118 – 140 (2014)

Paul, H., Luke, M. and Henning, F., "Combining Mechanical Interlocking, Force Fit and Direct Adhesion in Polymer–Metal-Hybrid Structures – Evaluation of the Deformation and Damage Behavior", Composites Part B, **73**, 158 – 165 (2015), DOI:10.1016/j.compositesb.2014.12.013

Paul, H., "Bewertung von langfaserverstärkten Kunststoff-Metall-Hybridverbunden auf der Basis des Verformungs- und Versagensverhaltens", PhD Thesis, Fakultät für Maschinenbau, Karlsruher Institut für Technologie, Karlsruhe (2013)

Ramani, K., Moriarty, B., "Thermoplastic Bonding to Metals via Injection Molding for Macro-Composite Manufacture", Polym. Eng. Sci., **38**, 870 – 877 (1998), DOI:10.1002/pen.10253

Ramani, K., Tagle, J., "Process-Induced Effects in Thin-Film Bonding of PEKEKK in Metal-Polymer Joints", Polym. Compos., **17**, 879 – 886 (1996), DOI:10.1002/pc.10681

Zhao, G., „Spritzgegossene, tragende Kunststoff-Metall-Hybridstrukturen", PhD Thesis, Lehrstuhl für Kunststofftechnik, Universität Erlangen-Nürnberg, Nüremberg (2002)

Date received: January 11, 2018
Date accepted: April 17, 2018

Bibliography
DOI 10.3139/217.3654
Intern. Polymer Processing
XXXIV (2019) 1; page 91 – 99

ISSN 0930-777X